Journal of Power Sources 225 (2013) 46–50

Contents lists available at SciVerse ScienceDirect

Journal of Power Sources

journal homepage: www.elsevier.com/locate/jpowsour

Short communication

Freestanding light scattering hollow silver spheres prepared by a facile sacrificial templating method and their application in dye-sensitized solar cells

Nafiseh Sharifi [a,b], Shabnam Dadgostar [c], Nima Taghavinia [a,b,*], Azam Iraji zad [a,b]

[a] Institute for Nanoscience and Nanotechnology, Sharif University of Technology, Tehran 14588, Iran
[b] Physics Department, Sharif University of Technology, Tehran 14588, Iran
[c] Physics Department, Humboldt University, Newtonstr. 15, D-12489 Berlin, Germany

HIGHLIGHTS

- Chemical deposition of silver on carbonaceous microspheres, which synthesized by a hydrothermal carbonization process.
- Calcination post-treatment of silvery carbonaceous microspheres to fabricate hollow silver microspheres.
- Protection of hollow silver spheres using SiO_2 shell overcoat before putting them in the electrolyte.
- Photon confinement in dye-sensitized solar cells using hollow silver spheres as freestanding light scattering centers.

GRAPHICAL ABSTRACT

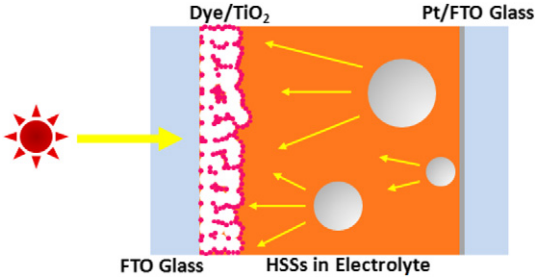

ARTICLE INFO

Article history:
Received 4 May 2012
Received in revised form
1 September 2012
Accepted 1 October 2012
Available online 18 October 2012

Keywords:
Metals
Chemical synthesis
Light scattering
Optical properties
Dye-sensitized solar cells

ABSTRACT

Hollow silver microspheres are synthesized in an easy and environmentally friendly process by a sacrificial templating method. Carbonaceous microspheres (CMSs) are used as hard templates, which have been synthesized previously by a hydrothermal carbonization process. Hollow silver spheres (HSSs) are synthesized by thermal removal of the core carbon component. The thickness of shell could be controlled by the concentration of precursors. Depending on the thickness, uniform or discontinuous shells are formed. The spheres are coated with SiO_2, and then added into the electrolyte of a dye solar cell. The enhancement of 50% is achieved in short-circuit current density (J_{SC}) due to the scattering and trapping of non-absorbed light inside of the sensitized TiO_2 film. In addition, 21% augmentation is observed in the photovoltaic power conversion efficiency (η).

1. Introduction

Dye-sensitized mesoporous nanocrystalline TiO_2 solar cells (DSCs) [1] have received considerable attention as a cost-effective alternative to silicon solar cells. DSCs work based on dye molecules chemisorbed onto the surface of a porous TiO_2 film, which inject electrons into TiO_2 upon photo-excitation. The pores of the

* Corresponding author. Institute for Nanoscience and Nanotechnology, Sharif University of Technology, Tehran 14588, Iran. Tel.: +98 21 6616 4532; fax: +98 21 6602 2711.
E-mail address: taghavinia@sharif.edu (N. Taghavinia).

0378-7753/$ – see front matter © 2012 Elsevier B.V. All rights reserved.
http://dx.doi.org/10.1016/j.jpowsour.2012.10.002

film are filled with a liquid electrolyte in which redox species transport holes from oxidized dye molecules to the counter electrode. The injected electrons also transport through the TiO_2 particle network to the collecting transparent conducting oxide substrate. The thickness of the film is decided based on two length scales of the cell: electron diffusion length in TiO_2, and the light penetration depth inside the dye-TiO_2 film [2,3]. The efficient light harvesting requires that the mesoporous film thickness is sufficiently large, in order to absorb all the incident photons. At the same time, it should be thin enough to minimize recombination and enable efficient carrier collection. This demonstrates that scattering reflectors are essential for efficient light absorption, in particular for thin and transparent films. TiO_2 large spherical particles are usually employed in order to scatter the light and increase the light pathway. It is usually applied as a scattering reflector film over the transparent mesoporous film [4]. In addition, thinner film is suggested to decrease the amount of dye up taking since dye is one of the factors that dominate the cost of DSCs.

In this study, carbonaceous microspheres (CMSs) were used as a template synthesized in an environmentally friendly approach, for production of hollow silver spheres (HSSs), aimed as light scattering centers in DSCs. Chemical precipitation of silver on CMSs was followed by calcination post-treatment at 300 °C to fabricate pure hollow silver microspheres. Silver has been preferred due to its high reflectance among different metals [5]. A SiO_2 shell overcoat was used as a corrosion protective shell as well as insulator to support HSSs. Then, a new design has been introduced in a way that the HSSs were mixed with the electrolyte, to apply as freestanding light scattering particles.

2. Experimental

2.1. Synthesis of HSSs

HSSs were prepared by chemical reduction/precipitation of silver on CMSs as sacrificial templates. CMSs were produced by hydrothermal carbonization of sucrose ($C_{12}H_{22}O_{11}$, Merck) as a precursor, in which the carbon-rich black solid is obtained as an insoluble product by heat-treating of an aqueous solution/dispersion of sucrose at 190 °C (under pressure) for 24 h [6].

A typical reduction/precipitation of silver on CMSs is similar to previously reported [7]: The starting silver ammonia aqueous solution was made by mixing 200 mM $AgNO_3$ (Acros) solution, 400 mM KOH solution (Wako) and ammonium hydroxide (Guangdong Guanghua, 25%). About 0.007 g of CMSs was dispersed in the mentioned solution by using sonication probe for 10 min. A solution of 280 mM sucrose ($C_{12}H_{22}O_{11}$, Merck) was then added to reduce silver on the surface of microspheres. This concentration was named [2*C*]. The other concentrations are denoted as [2*C*/*n*]; where *n* is the degree of dilution, compared to the mentioned concentration. The reaction was performed under mild magnetic stirring for 30 min to immobilize silver onto the microspheres. A rinsing process involving three cycles of washing was performed with water, and then precipitated products were dried on a hotplate at 90 °C for 3 h. In order to obtain hollow spheres from the core–shell composite particles as well as remove uncovered CMSs; and omit AgO as by-products, which are formed during reduction/precipitation of silver on CMSs, precipitated products were calcinated in air at 300 °C for 2 h. After this post-treatment, the dark gray initial powder consisting completely and partially silver-covered CMSs is converted to a silvery color due to omit of black CMSs. Fig. 1 shows the schematic procedure to prepare HSSs.

2.2. Coating of HSSs with SiO_2

Before incorporating the HSSs in the electrolyte, a SiO_2 shell was grown [8,9] to protect them from corrosion, as well as block any electrical contact with counter or working electrodes. The surface of HSSs was activated with 3-aminopropyltrimethoxysilane (Aldrich) to generate siloxy groups to silicate ion deposition. Then addition of sodium silicate ion (Merck) at supersaturated concentrations leads to an initial nanometer thick shell, and finally controlled precipitation of residual silicate by addition of ethanol creates a homogeneous shell.

2.3. Fabrication of DSCs

The amount of HSSs in the electrolyte is just 5% (w/v). To prepare working electrode, diluted Dyesol paste (DSL 18NR-T) was coated using doctor blade technique onto F-doped SnO_2 (NSG, sheet resistance 10 Ω sq^{-1}) glasses which the electrodes subjected to $TiCl_4$ (Merck) treatment at 70 °C for 30 min before and after coating of TiO_2 layer. All electrodes were sintered at 500 °C for 30 min. The counter electrodes with holes consist of platinum deposited on the conductive glasses (TEC, sheet resistance 7 Ω sq^{-1}). Having sensitized 0.6-μm films with Z907 ($RuLL'(NCS)_2$ (L = 2,2′-bipyridyl-4,4′-dicarboxylic acid; L′ = 4,4′-dinonyl-2,2′-bipyridine), Dyesol), the standard ruthenium complex sensitizer, the working and counter electrodes were assembled into a sandwich cell, and sealed with a hot-melt gasket of 25-μm thickness made of surlyn (Dyesol), they filled with the redox-active electrolyte (coded Z959) (mixture of HSSs and electrolyte) throughout the present study consisted of 1.0 M 1,3-dimethylimidazolium iodide (DMII), 30 mM I_2, 0.5 M *tert*-butylpyridine, and 0.1 M guanidinium thiocyanate (GNCS) in the mixed solvent of acetonitrile and valeronitrile (v/v, 85:15) [10]. All solvents and chemicals were obtained either from Aldrich or from BDH (India).

2.4. Characterization

The surface morphology was investigated using field emission scanning electron microscopy (FE-SEM, S4160) (Hitachi, Japan). Diffuse reflectance spectroscopy (DRS) analysis was performed using AvaSpec-2048TEC spectrometer. X-ray photoelectron spectroscopy (XPS) was performed using Al anode of a V.G. Microtech XR3E2 X-ray source and a concentric hemispherical analyzer (Specs

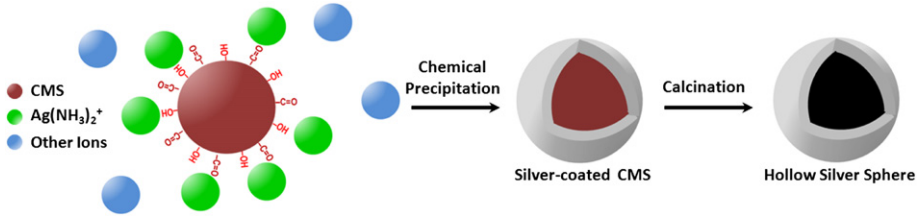

Fig. 1. Schematic procedure to prepare HSSs.

model EA10 plus). Photoelectrons were collected at a takeoff angle of 0° from the surface normal. A 450 W xenon light source (Oriel, USA) was used to characterize the cells. The spectral output of the lamp was matched in the region of 350–750 nm with the aid of a Schott K113 Tempax sunlight filter (Präzisions Glas & Optik GmbH, Germany) so as to reduce the mismatch between the simulated and true solar spectra to less than 2%. The current–voltage characteristics of the cell measured under these conditions were obtained by applying external potential bias to the cell and by measuring the generated photocurrent with a Keithley model 2400 digital source meter (Keithley, USA). The measurement of Monochromatic incident photon to current conversion efficiency (IPCE) was performed by using a similar data collection system but under monochromatic light obtained by passing the output of a 300 W xenon lamp (ILC Technology) through a Gemini-180 double monochromator (Jobin Yvon Ltd., U.K.).

3. Theoretical section

Light scattering by spherical particles can be analytically described by Mie resonance theory, in which the backscattering efficiency is given by the following equations, respectively:

$$Q_b = \frac{1}{x^2}\left|\sum_{n=1}^{\infty}(2n+1)(-1)^n(a_n - b_n)\right|^2$$

where $x = 2\pi r/\lambda$ is the size parameter, r is the radius of a metallic sphere, λ is the wavelength of light, and a_n and b_n are the complex Mie coefficients that can be calculated as:

$$a_n = \frac{\psi_n'(mx)\psi_n(x) - m\psi_n(mx)\psi_n'(x)}{\psi_n'(mx)\zeta_n(x) - m\psi_n(mx)\zeta_n'(x)}$$

$$b_n = \frac{m\psi_n'(mx)\psi_n(x) - \psi_n(mx)\psi_n'(x)}{m\psi_n'(mx)\zeta_n(x) - \psi_n(mx)\zeta_n'(x)}$$

where, m is the refractive index of a metallic sphere, and ψ and ζ are the Riccati–Bessel functions [11,12]. The thickness of HSSs (Fig. 2c) is sufficiently large (ca. 200 nm) to consider a HSS as a filled silver sphere. This is due to the very small light penetration depth into metals. The penetration depth of silver was calculated approximately 33 nm for $\lambda = 400$ nm and 25 nm for $\lambda = 700$ nm, based on the values of imaginary part of refractive index [13]. The reflectivity of a silver film with a thickness of 100 nm is about 90% [14,15], and for 200 nm thickness, 100% reflectance was obtained for the wavelengths between 400 and 700 nm. Therefore, the silver 200 nm-shells can be well assumed as a solid silver sphere. Thus a computer program based on the numerical calculation of the Mie efficiencies was utilized to present the backscattering efficiency vs. wavelength for a single sphere. Since CMSs have the sizes between 5 and 15 μm (Fig. 2a), spheres with different diameters (5, 10, and 15 μm) were assumed in the electrolyte with a refractive index of 1.5 [16] to show the contributions of the mentioned silver spheres in light backscattering in the range of 400–700 nm.

4. Results and discussion

4.1. Structural analysis

Fig. 2a shows the morphology of CMSs. They are spherical with diameters between 5 and 15 μm (inside Fig. 2a). Since a less-ordered medium is more effective to confine the light [17,18]; this size distribution could be more effective in photon confinement. For [*C*], uniform coatings of silver on CMSs are formed (Fig. 2b) because CMSs have a highly functionalized surface which can be easily deposited by silver complexes. The thicknesses of silver coatings are about 200 nm (inside Fig. 2d) and 100 nm (inside Fig. 2e) for [*C*] and [*C*/2], respectively. The thickness of HSSs (Fig. 2d) is large enough (ca. 200 nm) to have the highest reflectance for these spheres since 200-nm flat layer of silver presents 100% reflectance for wavelengths between 400 and 700 nm. Using full spheres of silver, and fabrication of HSSs with the thickness more than 200 nm, which obtained for [2*C*] (Fig. 2c) makes no additional advantage in terms of light reflection, while in full sphere of silver, consuming about eight times more material compared to hollow spheres. Therefore, HSSs could decrease the cost of DCSs rather than complete silver spheres.

Deposition of silver on CMSs is accompanied by precipitation of minor AgO as by-product, which is decomposed to metallic silver by post-treatment [19]. CMSs were removed from the inner part of the spheres by burning at 300 °C for 2 h, and then silver microspheres remained. As seen in Fig. 2d, a hole is created on HSS, which allows mainly CO_2 and H_2O as burning by-products out. In case of [*C*/2] and [*C*/4], post-treatment results in a non-continuous film consisting separated formless particles connected to each other.

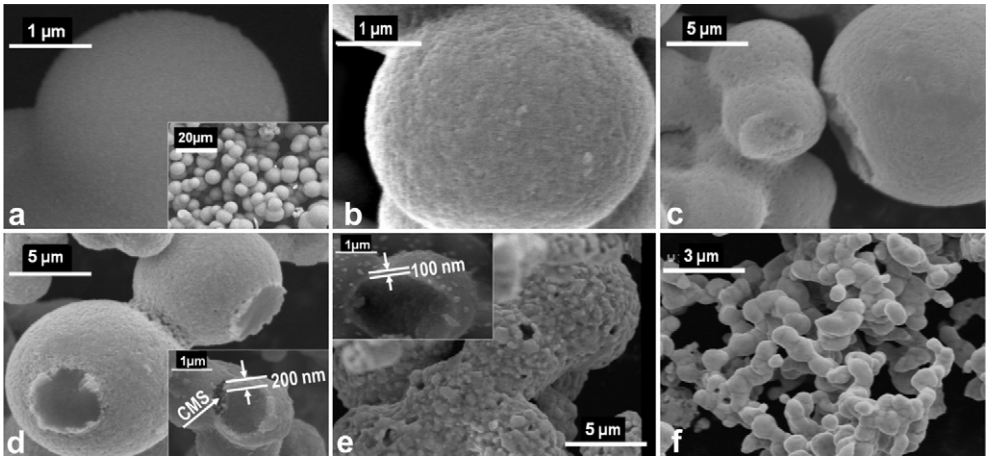

Fig. 2. FE-SEM images of (a) CMSs, silver-deposited CMSs with concentration of (b and inside d) [*C*] and (inside e) [*C*/2]; annealed silver-deposited CMSs with concentration of (c) [2*C*], (d) [*C*], (e) [*C*/2], and (f) [*C*/4] at 300 °C for 2 h.

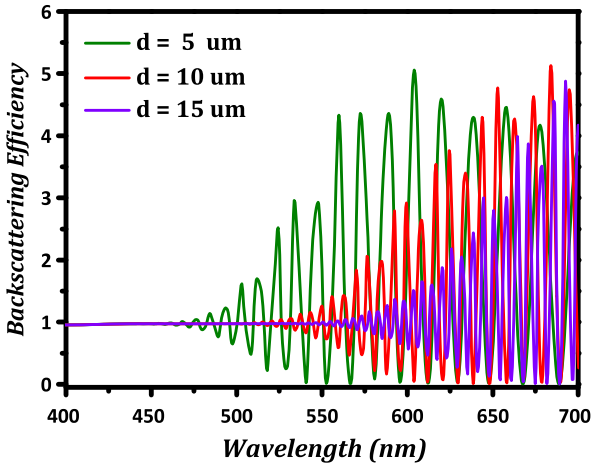

Fig. 3. Backscattering efficiency from a single silver sphere with diameters of 5, 10 and 15 μm.

Due to the presence of voids between particles, the created burning gases are exhausted through the voids (Fig. 2e and f). Although both [*C*/2] and [*C*/4] have Granular structures and [*C*/2] appears in spherical shapes (Fig. 2e), granular structures of [*C*/4] are not spherical and they have disorder shapes (Fig. 2f).

4.2. Size effect on the backscattering efficiency

In spite of the poly-disperse collection of particles which can be found in the experimental synthesis processes, it is often sufficient to study simpler systems for understanding the elementary phenomena occurring in them. Therefore, to evaluate the contribution of spheres with different sizes in backscattering efficiency from a HSS, a silver sphere with diameter of 5, 10, and 15 μm was calculated and plotted in Fig. 3. The backscattering efficiency is a function of the incident wavelength and size. A series of regular maxima and minima occur due to the interference between the incident and backward scattered light, which are smoothed out in the real, multiple reflection case. The increase in the size causes that oscillations move toward long wavelength. The backscattering efficiency increases in the wavelength range of 400–700 nm as the size decreases. Therefore among spheres with different sizes from 5 to 15 μm, sphere with smaller sizes have more contribution in the enhancement of backscattering efficiency in the mentioned region.

4.3. Optical and chemical state characteristics

DRS was used to characterize the reflectance properties of HSSs (Fig. 4a). The trend of spectra for four concentrations is similar. They increase as the light goes from 400 nm to 700 nm, which is typical for scatterers. HSSs with [2*C*] and [*C*] have similar reflectance and the highest reflectance belongs to them. For HSSs with [*C*/2], the weak absorption band at around 400 nm could be attributed to the surface plasmon resonance of the silver nanoparticles (Fig. 2e) which it causes the attenuation of the reflectivity. By increasing the concentration, the reflectance enhances from 25% to 50%, 77% and 78% at around 650 nm at which the dye has no considerable absorbance (Fig. 5b). Since hollow spheres made by concentration [*C*] do not show surface plasmon absorption and have higher reflectivity, as well as from the view point of cost, these HSSs consume lower materials in comparison with [2*C*]; they were employed to modify a conventionally fabricated DSC.

In order to determine the chemical states of the surface of these HSSs, XPS analysis was used. The C 1s peak of hydrocarbon contamination, at a binding energy of 284.5 eV was used as an energy reference. Fig. 4b shows the XPS spectra of the HSSs in the Ag 3d core level region. In order to investigate the presence of any silver oxide, the Ag $3d_{5/2}$ peaks were deconvoluted into two components. These two components have binding energies of 368.2 eV for pure silver [20] and 367.5 eV for Ag_2O [21]. The oxide component is 27.8% of the total peak. The reason for this oxidation could be attributed to a competition among (i) thermal oxidation of silver in air and (ii) the reducing property of the CMSs as well as (iii) the native thermal decomposition of silver oxide [22].

4.4. Photovoltaic and optical characteristics

As displayed in Fig. 5a, the non-modified DSC shows J_{SC} of 1.63 mA cm^{-2}, V_{OC} of 795 mV; and a fill factor of 0.76. The corresponding photovoltaic power conversion efficiency (η) was 0.99 ± 0.05%. The modified device with HSSs gives 1.20 ± 0.06% efficiency with $J_{SC} = 2.45$ mA cm^{-2}, $V_{OC} = 726$ mV, and fill factor of 0.66. Although open circuit voltage and fill factor decrease by incorporating of HSSs, ca. 50% enhancement in J_{SC} causes 21% enhancement in the efficiency. The improvement in the current density is due to the scattering property of the spheres inside the electrolyte, which enhances the light harvesting by exciting more dyes and injecting more electrons into the TiO_2 conduction band.

IPCE of devices plotted in Fig. 5b as a function of excitation wavelength supports the light trapping effect of HSSs and

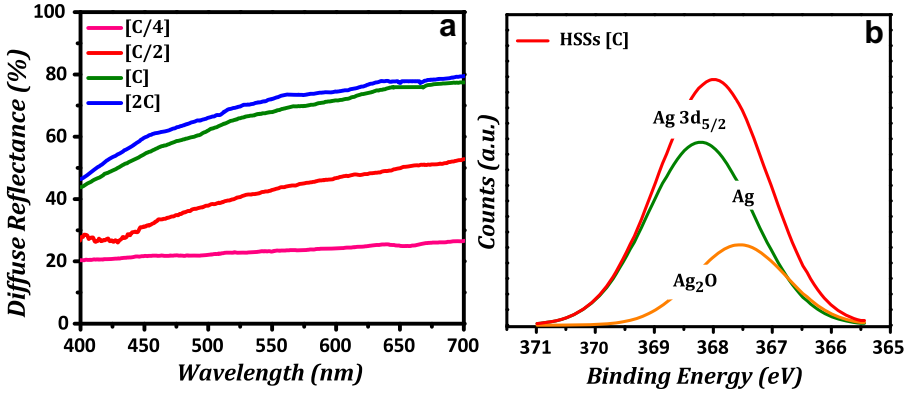

Fig. 4. (a) Diffuse reflectance spectra of annealed silver-deposited CMSs with concentrations of [*C*/4], [*C*/2], [*C*] and [2*C*] (b) XPS spectra of HSSs with concentration of [*C*]. It shows the silver core level region.

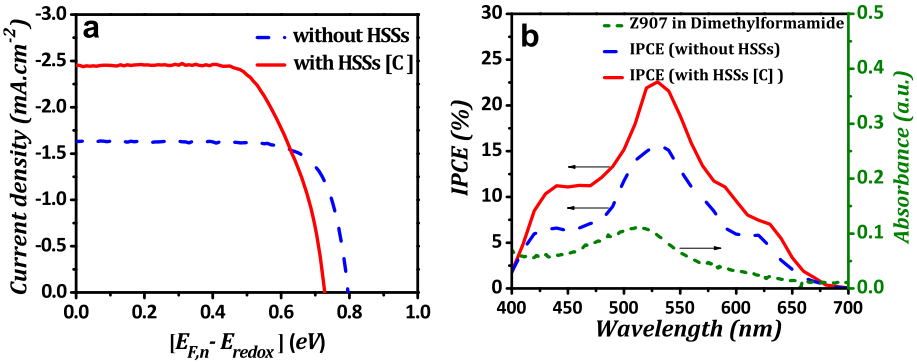

Fig. 5. (a) *J–V* characteristics of devices with, and without HSSs under illumination with standard AM 1.5 simulated sunlight (100 mW cm^{-2}). (b) IPCE spectra of cells, and absorbance of Z907 in dimethylformamide.

consequently enhancement of J_{SC}. The maximum value of IPCE occurs at around 530 nm, which corresponds to the absorption peak for Z907. This value increases from 16% to 24% by incorporation of spheres. In addition, the enhancement in IPCE is not limited to specific wavelengths as well as it occurs in the range of wavelengths which the dye absorbs light due to the fine reflectance of HSSs with [*C*] concentration in this range (Fig. 4a).

5. Conclusion

In summary, we have demonstrated a facile method for the synthesis of HSSs using CMSs as sacrificial templates. CMSs were prepared from cheap natural precursors using environmentally friendly processes. The calcinations post-treatment favored the formation of compact silver shells, subsequently, resulting in the formation of HSSs. Having incorporating of these freestanding spheres in the dye-sensitized solar cell, they act as light trapping centers to augment J_{SC} and η by ca. 50% and 21%, respectively. In addition, according to Mie calculation, for spheres between 5 and 15 μm, smaller ones accomplish more contribution to enhance the photovoltaic efficiency.

Acknowledgment

The authors would like to acknowledge Dr. Takeru Bessho for his willing collaboration.

References

[1] B. O'Regan, M. Grätzel, Nature 353 (1991) 737.
[2] Y. Tachibana, K. Hara, K. Sayama, H. Arakawa, Chem. Mater. 14 (2002) 2527.
[3] M. Grätzel, Inorg. Chem. 44 (2005) 6841.
[4] S. Ito, T.N. Murakami, P. Comte, P. Liska, C. Grätzel, M.K. Nazeeruddin, M. Grätzel, Thin Solid Films 516 (2008) 4613.
[5] H.W. Edwards, R.P. Petersen, Phys. Rev. 50 (1936) 871.
[6] S.M. Sevilla, A.B. Fuertes, Chem. Eur. J. 15 (2009) 4195.
[7] N. Sharifi, N. Taghavinia, Mater. Chem. Phys. 113 (2009) 63.
[8] L.M. Liz-Marzan, M. Giersig, P. Mulvaney, Langmuir 12 (1996) 4329.
[9] T. Ung, L.M. Liz-Marzan, P. Mulvaney, Langmuir 14 (1998) 3740.
[10] L. Giribabu, T. Bessho, M. Srinivasu, C. Vijaykumar, Y. Soujanya, V.G. Reddy, P.Y. Reddy, J. Yum, M. Grätzel, M.K. Nazeeruddin, Dalton Trans. 40 (2011) 4497.
[11] C.F. Bohren, D.R. Huffman, Absorption and Scattering of Light by Small Particles, Wiley-Interscience, New York, 1983, p. 101, 122.
[12] O. Peña, U. Pal, Comput. Phys. Commun. 180 (2009) 2348.
[13] E.D. Palik, Handbook of Optical Constants of Solids, second ed., Academic, New York, 1997, p. 356.
[14] A. Giannattasio, I.R. Hooper, W.L. Barnes, Opt. Express 12 (2004) 5881.
[15] X. Sun, R. Hong, H. Hou, Z. Fan, J. Shao, Thin Solid Films 515 (2007) 6962.
[16] J. Ferber, J. Luther, Sol. Energy Mater. Sol. Cells 54 (1998) 265.
[17] H. Cao, J.Y. Xu, D.Z. Zhang, S.H. Chang, S.T. Ho, E.W. Seelig, X. Liu, R.P.H. Chang, Phys. Rev. Lett. 84 (2000) 5584.
[18] Q. Zhang, C.S. Dandeneau, K. Park, D. Liu, X. Zhou, Y. Jeong, G. Cao, J. Nanophotonics 4 (2010) 041540.
[19] N. Sharifi, F. Tajabadi, N. Taghavinia, Int. J. Hydrogen Energy 35 (2010) 3258.
[20] Y. Abe, T. Hasegawa, M. Kawamura, K. Sasaki, Vacuum 76 (2004) 1.
[21] Y. Chiu, U. Rambabu, M. Hsu, H. Shieh, C.Y. Chin, H.H. Lin, J. Appl. Phys. 94 (2003) 1996.
[22] G.I.N. Waterhouse, G.A. Bowmaker, J.B. Metson, Phys. Chem. Chem. Phys. 3 (2001) 3838.